Cell Reports
Article

Cell PRESS
Open ACCESS

Bat-Derived Influenza Hemagglutinin H17 Does Not Bind Canonical Avian or Human Receptors and Most Likely Uses a Unique Entry Mechanism

Xiaoman Sun,[1,3,8] Yi Shi,[1,2,8] Xishan Lu,[1,5] Jianhua He,[6] Feng Gao,[4] Jinghua Yan,[1] Jianxun Qi,[1] and George F. Gao[1,2,3,7,*]
[1]CAS Key Laboratory of Pathogenic Microbiology and Immunology, Institute of Microbiology, Chinese Academy of Sciences, Beijing 100101, China
[2]Research Network of Immunity and Health, Beijing Institutes of Life Science, Chinese Academy of Sciences, Beijing 100101, China
[3]University of Chinese Academy of Sciences, Beijing 100049, China
[4]Laboratory of Noncoding RNA, Institute of Biophysics, Chinese Academy of Sciences, Beijing 100101, China
[5]College of Veterinary Medicine, China Agricultural University, Beijing 100193, China
[6]Shanghai Institute of Applied Physics, Chinese Academy of Sciences, Shanghai 201204, China
[7]National Institute For Viral Disease Control and Prevention, Chinese Center For Disease Control and Prevention, Beijing 102206, China
[8]These authors contributed equally to this work
*Correspondence: gaof@im.ac.cn
http://dx.doi.org/10.1016/j.celrep.2013.01.025

SUMMARY

A new influenza-like virus genome (H17N10) was recently discovered in bats and offers a new perspective about the origin and evolution of influenza viruses. The viral envelope glycoprotein hemagglutinin (HA) is responsible for influenza virus receptor binding, fusion, and entry into the cell; therefore, the structure and function of HA H17 was characterized. The 2.70 Å resolution crystal structure revealed that H17 has a typical influenza A virus HA fold, but with some special features, including a distorted putative sialic acid (SA) binding site and low thermostability. No binding to either the canonical human α2,6 SA-linkage or avian α2,3 SA-linkage receptor was observed. Furthermore, H17 glycan binding was not detected using a chip covering more than 600 glycans. Our results demonstrate that H17 is unique among characterized HAs and that the bat-derived influenza virus may use a different entry mechanism compared to canonical influenza viruses.

INTRODUCTION

Influenza virus is one of the most important pathogens that exert a dramatic impact on public health and the global economy (Medina and García-Sastre, 2011). There are three types of influenza viruses: A, B, and C. Among them, influenza A viruses are the major pathogens responsible for seasonal flu and occasional pandemics (Gao and Sun, 2010; Guan et al., 2010; Liu et al., 2009; Neumann et al., 2009; Sun et al., 2010). Recently, a distinct lineage (H17N10) of influenza A virus derived from bats, from which only the genome was identified, was reported to possess the potential to reassort with human influenza viruses (Tong et al., 2012). This discovery provided novel insights into the origin and evolution of influenza A viruses beyond the predominant hypothesis of waterfowls/shorebirds as the primary natural reservoir (Webster et al., 1992). However, the putative products of the eight gene segments of the H17N10 virus genome are unique among all known influenza A viruses at the primary sequence level (Tong et al., 2012). Recently, our group and the Wilson group at Scripps revealed that the bat-derived N10 neuraminidase-like molecule displays a canonical sialidase fold in general but lacks sialidase activity (Li et al., 2012; Zhu et al., 2012), raising doubts about the ability of the bat-derived genome to function as a live virus. Hence, structural and functional characterizations of other H17N10 proteins are ongoing in an effort to increase our overall understanding of the biology of this unusual viral genome.

The hemagglutinin (HA) of influenza A/B virus is responsible for virus attachment, entry, and fusion. Before the discovery of the bat-derived H17N10 virus genome, there were 16 known HA subtypes that could be phylogenetically divided into two groups: group 1 contains H1, H2, H5, H6, H8, H9, H11, H12, H13, and H16; and group 2 contains H3, H4, H7, H10, H14, and H15 (Air, 1981; Gamblin and Skehel, 2010; Nobusawa et al., 1991). HA is a trimer of identical subunits, each of which contains two polypeptides (HA1 and HA2) created by enzymatic cleavage of a single precursor protein, HA0. Initiation of virus infection involves multiple HAs binding to their receptors, sialic acids (SAs) terminating on the carbohydrate chains of cell-surface glycoproteins and glycolipids (Gambaryan et al., 1997; Sauter et al., 1989; Takemoto et al., 1996). There are two main forms of receptors for influenza A viruses: the α2,6 SA-linkage galactose receptor for mammalian cells and the α2,3 SA-linkage galactose receptor for avian cells (Gambaryan et al., 1997; Sauter et al., 1989; Takemoto et al., 1996). After virus attachment and entry into the cell through endocytosis, the HAs are activated to exert membrane fusion under low-pH conditions in the endosome through large conformational rearrangements (Bullough et al., 1994; Harrison, 2008).

In the present study, we examined the receptor binding properties of the bat-derived H17 protein and report its crystal structure. Prior primary sequence analysis shows that the H17 protein has 45% sequence identity to the other HAs from the 16 known influenza A subtypes, which is similar to the 49% mean identity observed among those known subtypes (Tong et al., 2012). However, our results show that the H17 protein does not bind to the canonical human or avian receptors due to a conformation-altered pseudo-receptor-binding site. Our further experiments demonstrate that no H17 glycan binding could be detected using a chip covering more than 600 glycans. Furthermore, H17 displayed an altered trypsin susceptibility and instability even at pH 8.0 (for canonical HAs, this can only be observed at low pH), which may result from an exposed fusion peptide and contorted trimerization of HA monomers as observed in the crystal structure. Together with our and the Wilson group's recent work on N10 (Li et al., 2012; Zhu et al., 2012), these results indicate that the bat-derived influenza virus might use an alternative cell-entry mechanism.

RESULTS

Soluble H17 Does Not Bind the Canonical SA Receptors

The sequence encoding the ectodomain of the H17 protein from influenza virus A/little yellow-shouldered bat/Guatemala/060/2010 (H17N10) was cloned and expressed using a baculovirus expression system, as previously described (Zhang et al., 2010). The receptor binding properties of the H17 protein were investigated by surface plasmon resonance (SPR) technology, Madin-Darby canine kidney (MDCK) cell binding assays, and glycan microarrays. Interestingly, SPR experiments revealed that H17 protein does not bind to canonical α2,3-linkage or α2,6-linkage sialylated glycans. As a positive control, we showed that the H5 protein from the highly pathogenic avian influenza virus A/BhGoose/QH/1/05 bound to α2,3-linkage sialylated glycans (Figures 1A and 1B). ELISA-based MDCK cell binding assays also indicated that, unlike H5, H17 does not bind to MDCK cells (Figure 1C), the surface of which is rich in sialylated glycans receptors for viral attachment.

Next, large-scale glycan microarray analysis was performed to examine the receptor binding properties of the H17 protein. This glycan microarray consists of >600 glycans, including natural sialosides (α2,3-linkage, α2,6-linkage, α2,8-linkage, and mixed linkage) and other glycans that may be relevant to influenza biology. As a positive control, the H3 protein from the 1968 Hong Kong pandemic virus displayed significant avidity to α2,6-linkage sialylated glycans (Figure 1D). Extraordinarily, the H17 protein did not display obvious avidity to any glycans on the microarray (Figure 1D; Table S1), indicating that the bat virus might use other receptors for infection if it truly produced a live virus.

Biochemical and Biophysical Characterization of Soluble H17

During virus infection, the HA protein has two main functions: virus attachment and virus fusion (Skehel and Wiley, 2000). The receptor binding site of HA is responsible for virus attachment, and different receptor binding specificities determine the host range of the virus (i.e., host shift) (Skehel and Wiley, 2000). Following attachment, virus membrane fusion is essential for the release of the virus genome into the cells, initiating virus replication in the host cells. Cleavage of the initially synthesized HA0 precursor into a disulfide bond-linked HA1/HA2 form must occur prior to the activation of membrane fusion and hence infectivity (Garten and Klenk, 1999; Skehel and Wiley, 2000). Upon incubation at fusion pH, the cleaved HA protein aggregates and becomes susceptible to trypsin digestion, undergoing irreversible conformational changes required for the membrane fusion activity (Skehel et al., 1982). The products of digestion can be separated by sucrose density gradient centrifugation into aggregated HA2 and a soluble HA fraction that reveals cleavage within HA1 at the K27 and R224 positions (Skehel et al., 1982). Surprisingly, the H17 precursor protein was susceptible to trypsin digestion at both pH 8.0 and low pH (5.0) and was digested into various HA1 fragments in a time-dependent manner (Figures 2A and 2B). In contrast, control H3 precursor proteins were digested into normal HA1 and HA2 fragments at pH 8.0, which are clearly present as two bands by SDS-PAGE analysis (Figure 2C). However, after low-pH (5.0) incubation, the cleaved H3 protein displayed HA1 fragmentation (Figure 2D), similar to the H17 protein at pH 8.0. Furthermore, temperature-dependent circular dichroism (CD) spectroscopic experiments revealed that H17 has a lower thermostability than the H1, H2, H3, H5, and H16 proteins tested (Figure 2E). Both the trypsin digestion and CD spectroscopy results imply that the H17 protein has unique biochemical and biophysical properties. Moreover, we were also able to confirm that the H17 precursor protein exists as a trimer in solution through a sedimentation-velocity analytical ultracentrifugation assay (Figure 2F).

Overall Structure of H17

The H17 structure was solved by molecular replacement at a resolution of 2.7 Å using H16 (Protein Data Bank [PDB] ID code 4F23) as a search model (Table S2) (Lu et al., 2012). The crystal structure exhibits a classical homotrimer structure with two distinct domains: a globular domain and a stem domain (Figure 3A). Further analysis revealed that the H17 structure solved here exists as a cleaved HA1/HA2 form, although it was expressed as the HA0 form in the baculovirus system. In order to confirm this, we isolated H17 crystals and checked for proteolytic processing by SDS-PAGE (Figure S1). Furthermore, N-terminal amino acid sequencing of the HA2 band from the SDS-PAGE revealed that the first five amino acids of HA2 were GLFGA (Figure S1). Thus, the cleavage occurred at the authentic site. The membrane-distal globular domain contains the receptor binding subdomain and the vestigial esterase subdomain, responsible for virus attachment. The membrane-proximal stem domain consists of HA2 and two segments of HA1 (i.e., residues 1–55 and 275-329) responsible for virus fusion. There are five predicted N-linked glycosylation sites (N17, N114, N288, N472, and N482); however, only two sites (N17 and N114) are observed with glycans in the current H17 structure.

Tong et al. (2012) recently reported that the H17 HA gene clusters with group 1 HA gene sequences, which is demonstrated here through the phylogenetic tree (Figure 3B). This indicates that the H17 structure might resemble the structures of group

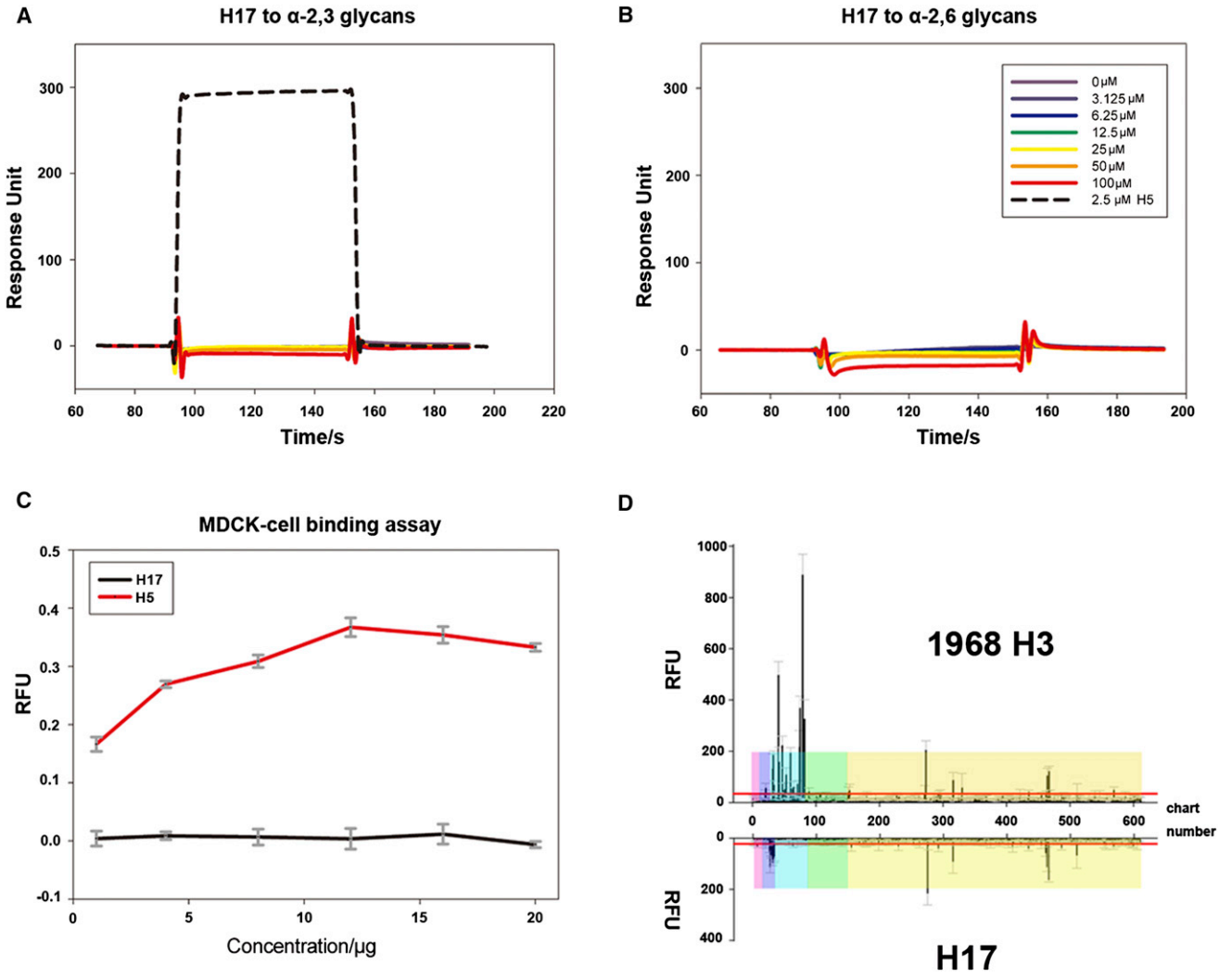

Figure 1. H17 Protein Does Not Bind to Canonical SA Receptors

(A and B) SPR of H17 protein binding to α2,3-linked and α2,6-linked receptors at a series of concentrations from 0 to 100 μM. As a positive control, SPR of QH05-H5 protein binding to α2,3-linked receptor at a concentration of 2.5 μM was performed (dotted line in A).

(C) ELISA-based MDCK cell binding assay. H17 did not bind to MDCK cells, and as a positive control, the QH05-H5 protein bound to MDCK cells well.

(D) Glycan microarray analyses of the 1968 Hong Kong H3 protein (upper) and the H17 protein (lower). Binding to different types of glycans on the array is highlighted, where magenta represents Neu5Gc, blue represents α2,8-ligands, cyan represents α2,6-ligands, green represents α2,3-ligands, and yellow represents other glycans. The H3 protein displayed a good avidity to α2,6-ligands, but the H17 protein showed no obvious avidity to any of the glycans. Error bars represent SD of the mean.

See also Table S1.

1 HAs rather than those of group 2. The superimposition of other HA structures onto the H17 monomer by means of their HA2 domains (root-mean-square deviation [rmsd] in Table S3) shows that H17 is most closely related to the 2009 pandemic H1 subtype (2009 pH1N1) and 1957 Singapore H2 subtype (rmsd = 0.684 and 0.694, respectively), whereas the human H3 subtype and the avian H16 subtype are the most divergent (rmsd = 1.170 and 1.166, respectively). Based on its HA1 domain, H17 is most closely related to the avian H16 subtype (rmsd = 1.358), whereas the avian H14 subtype is the most divergent (rmsd = 2.631). However, with regard to the receptor binding region (R region), H17 is most closely related to the avian H14 subtype (rmsd = 0.994,) and the H5 subtype is the most divergent (rmsd = 1.291).

Previously solved HA structures demonstrate that there are group-specific features at sites where extensive conformational changes occur for HA activation, including the conformation of the interhelix loop and the rigid body orientation of the globular domain (Figures 3C and 3D). H17 displays a similar interhelix loop conformation to the HAs from group 1, which is consistent with the phylogenetic analysis. Superimposition with other solved HA structures by means of the long central α helices of HA2 revealed that the globular domains fall into three groups: group 1, including H1, H2, H5, and H9; group 2, including H3,

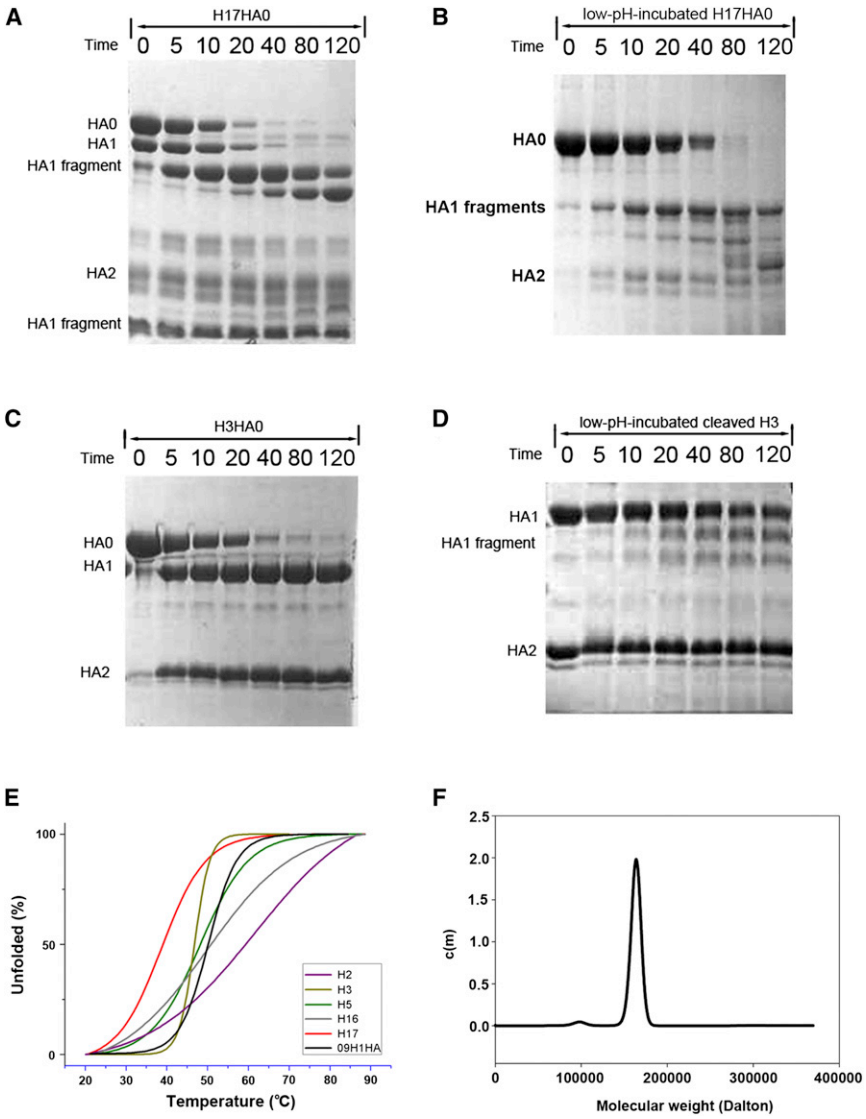

Figure 2. Biochemical and Biophysical Characterization of the Soluble H17 Protein

(A–D) Trypsin susceptibility assays of the soluble H17 protein (A), 1968 Hong Kong H3 protein (B), low-pH-incubated H17 protein (C), and H3 protein (D). The H17 protein can be digested into different HA1 fragments and one HA2 fragment at pH 8.0. As a representative of characterized HA proteins, the 1968 Hong Kong H3 protein can be digested into one HA1 fragment and one HA2 fragment. The low-pH-incubated (pH 5.0) H17 and H3 proteins can be digested into different HA1 fragments and one HA2 fragment, similar to the H17 protein at pH 8.0.

(E) Thermostability analyses of the H17 protein and other characterized HA proteins (09H1, H2, H3, H5, and H16). Temperature-dependent CD spectroscopic experiments revealed that the H17 protein has a much lower midpoint transition temperature (T_m = ~40°C) than other known HA proteins (T_m = ~50°C).

(F) Sedimentation-velocity analytical ultracentrifugation of H17 protein. The H17 protein exists as a trimer (~180 kDa) in solution.

H7, and H14; and group 3, consisting of H16 and H17. These differences may result from subtle variation in the interhelix loops among different HA subtypes (Figure S2) and could signify different mechanisms during HA activation.

Structural Basis for the Lack of Canonical SA Receptor Binding

The HA receptor binding site consists of two parts: the edge and base. The edge portion is formed by three secondary elements (the 130-loop, the 190-helix, and the 220-loop), and the base portion is formed by four conserved residues (Y98, W153, H183, and Y195). These two portions usually form a shallow cavity to accommodate sialylated glycans, as illustrated by the representative H1 subtype in Figure 4A. There is no obvious cavity in the putative receptor binding site of H17; the site is substituted by a negatively charged region (Figures 4B and 4C). Detailed analysis of amino acid interactions revealed that residues D136, H226, D228, and Q190 in H17 tighten the 130-loop, 190-helix, and 220-loop together to form a flat surface through a tight hydrogen bond and salt bridge network (Figure 4D). This flat surface provides a much lower possibility for canonical SA receptor binding in the H17 protein.

SA is bound similarly in all HAs through hydrophobic interactions and hydrogen bonds with the 130-loop as well as with the conserved residues in the base of the binding site. For example, multiple hydrogen bonds are formed in human H3 HA (Eisen et al., 1997). These include the negatively charged SA carboxylate group with both side chains of residue 136 (usually T or S in all known HA subtypes except H17; see Figure S3) and the main-chain amide of residue 137 (Figure 4E); the SA acetamido nitrogen with the main-chain carbonyl of residue 135 (Figure 4E); the SA 8-OH group with the OH group of Y98; and the SA 9-OH with H183 (Eisen et al., 1997; Weis et al., 1988). In addition, the methyl group of the acetamido substituent forms a hydrophobic interaction with W153 (Eisen et al., 1997; Weis et al., 1988). However, in H17, the corresponding residue 136 is a negatively charged aspartate (D136), which has an electrostatic repulsion with the negatively charged carboxylate group of SA (Figure 4F). Additionally, residue 98 is a hydrophobic phenylalanine (F) in H17 (usually Y in other HAs) and F98 cannot form hydrogen bond with SA, further decreasing the potential for H17 to bind SA. In conclusion, these altered amino acids in the putative receptor binding site rule out the possibility of canonical SA receptor binding by H17.

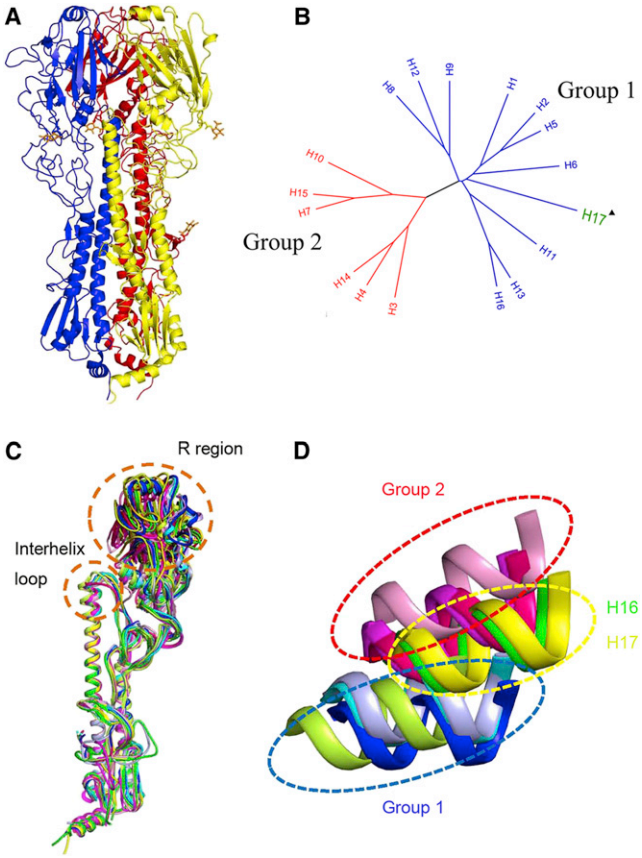

Figure 3. Overall Crystal Structure of the H17 Protein and Comparison with Other Solved HA Subtype Structures

(A) Overall structure of the H17 protein. H17 adopts a typical HA trimer structure, containing a membrane-distal globular domain and membrane-proximal stem domain.

(B) Phylogenetic tree showing that H17 belongs to group 1.

(C and D) Comparison of the H17 monomer with other solved HA subtype structures (H1, light blue; H2, cyan; H3, magenta; H5, blue; H7, pink; H9, limon; H14, hot pink; H16, green; and H17, yellow). The interhelix loop of the H17 structure displays a similar conformation to the group 1 HAs (H1, H2, H5, H9, and H16), which is distinct from the group 2 HAs (H3, H7, and H14). The rigid body orientation of the globular domain in the H17 structure is similar to that of the H16 subtype, by means of superimposition through the long helix of HA2. They are located between other group 1 HAs and group 2 HAs.

See also Figures S1 and S2, and Tables S2 and S3.

Special Features of the Exposed Fusion Peptide

In all solved cleaved HA structures, the N-terminal HA2 fusion peptide inserts into an electronegative cavity composed of different HA monomers (Figure 5A) and forms up to five hydrogen bonds between the backbone amide group of G1 and conserved HA2 ionizable residues (D109 and D112) (Chen et al., 1998). As discussed above, the H17 protein exhibited strong trypsin susceptibility and instability; therefore, we examined the cleavage site in the H17 structure in detail. Extraordinarily, an exposed fusion peptide was observed in the cleavage site (Figure 5B). Unambiguous electron density was seen from the fifth residue (A5) of the fusion peptide (Figure S4), but the first four residues (G1, L2, F3, and G4) were not seen in the H17 structure (Figures 5C and 5D). Although we cannot observe the first four residues, different orientations of A5 in the H17 structure and other known cleaved HA structures helped to confirm that the fusion peptide does not insert into the cavity. A similar exposed fusion peptide has been observed previously in the hemagglutinin-esterase fusion (HEF) protein of influenza C viruses (Rosenthal et al., 1998) (Figures 5E and 5F), but until now has not been seen in HA proteins of influenza A or B viruses.

To elucidate why the fusion peptide does not insert into the cavity, we carefully examined the residues around the cavity but failed to find any particular residues that may be responsible for this phenomenon. However, further analysis of the HA trimerization model revealed that the H17 trimer packs much more tightly than the representative H3 trimer (Figure S5). In all known cleaved structures, the fusion peptide forms a hydrophobic core (mainly constituted by the F3 residue) in the center of the HA trimer (Figure S5), which helps to stabilize HA trimerization. However, in the H17 structure, the HA monomers pack more tightly than in the representative H3 structure due to contorted trimerization (Figure S5), resulting in a narrower cavity that precludes the entry of the fusion peptide. Furthermore, lack of a hydrophobic core formed by the fusion peptide could explain the observed instability of the H17 protein.

Conserved Hydrophobic Groove for Cross-reactive HA2 Antibodies in H17

The HA of influenza virus is a major target for vaccine design (Xuan et al., 2011). Recently, several cross-reactive HA2 neutralizing antibodies have been identified to neutralize a wide spectrum of influenza A viruses by binding to highly conserved epitopes in the stem region of HA (Corti et al., 2011; Ekiert et al., 2009, 2011; Sui et al., 2009). Among these antibodies, FI6 has been reported to bind almost all the HA subtypes (H1 to H16) (Corti et al., 2011), with the exception of the recently reported H17 protein, which was not tested. The crystal structure of FI6-09H1 complex revealed that the antibody targets a shallow hydrophobic groove on the F subdomain of the HA, where the sides of the groove are formed by the residues from the A helix of HA2 (including L38, T41, I45, and I48) and parts of two strands of HA1 (including V40 and T318), and the HA2 turn (including W21), encompassing residues 18 to 21 (Figure 6A). In H17 HA, a similar hydrophobic groove is observed but with three different residues: A40 (V), K38 (L), and V45 (I) (Figure 6B). Thus, we deduce that those cross-reactive HA2 neutralizing antibodies, like FI6, might bind to the H17 protein.

DISCUSSION

Here, we demonstrated that the bat-derived influenza virus H17 protein does not bind to canonical human or avian receptors based on multiple lines of evidence, including SPR experiments, MDCK cell binding assays, and glycan microarray analysis. This lack of canonical receptor binding is likely due to specific structural features in the putative receptor binding site of H17 HA. In the H17 structure, there is no obvious cavity to accommodate the sialylated glycans due to strong interactions among three secondary elements (130-loop, 190-helix, and 220-loop) through a hydrogen bond and salt bridge network formed by residues

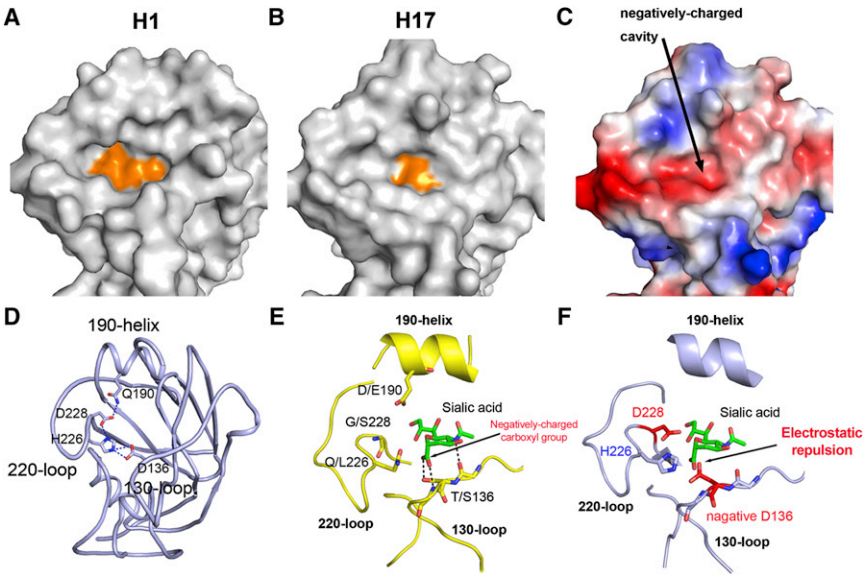

Figure 4. Structural Basis of the Lack of H17 Binding to Canonical SA Receptors

(A and B) Surface representations of the receptor binding cavity in typical H1 (PDB ID code: 3AL4) and H17 structures. The typical H1 subtype displays a clear shallow receptor binding cavity, whereas H17 does not have an obvious cavity. The bottoms of the cavity are marked in orange.

(C) Electrostatic potential maps of the receptor binding sites from the H17 structure. In the H17 structure, the receptor binding cavity is negatively charged.

(D) Cartoon diagram of the receptor binding site in the H17 structure. The key residues D136, Q190, H226, and D228 tightly link the 130-loop, 190-helix, and 220-loop together through a hydrogen bond and salt bridge network. The hydrogen bonds and salt bridges are shown in a dash line.

(E) Cartoon diagram of SA binding in the receptor binding site of the representative H3 structure. The SA forms three hydrogen bonds with the 130-loop, and the negatively charged carboxylate group forms a strong bond with the T/S136 residue.

(F) Model diagram of the putative SA binding site of the H17 structure. The negatively charged D136 residue has an electrostatic repulsion with the negatively charged carboxylate group of the SA, which impedes SA binding in H17.

See also Figure S3.

D136, Q190, H226, and D228. Furthermore, the negatively charged D136 in the 130-loop (all canonical influenza HAs have an uncharged threonine or serine at this position) could result in an electrostatic repulsion with the negatively charged carboxylate group of SA, which is unfavorable for SA receptor binding. Moreover, the residue 98 (usually a conserved tyrosine) in the base of the receptor-binding site is a phenylalanine in H17, which could also affect the SA receptor binding capacity. Thus, these five key residues likely contribute to the lack of SA receptor binding by H17 and make the putative binding cavity a much smaller, pseudo binding site.

Nevertheless, the overall secondary structure architecture of the receptor binding site in H17 is similar to other known HA subtypes. In solved HA structures, the corresponding residues are Y98, T/S136, D/E190, Q/L226, and G/S228. Substitution of these residues confirms their importance for the avian or human SA receptor preference (Gamblin and Skehel, 2010). For example, in both H2 and H3 HAs, Q226L and G228S substitutions are responsible for the switch between avian and human receptor binding specificities, whereas in H1 HA, different combinations of substitutions at residues 190 and 225 are important for the SA binding preference. Thus, it is possible that substitutions at these key residues may be able to induce H17 to bind SA receptors, but no binding was observed in the H17 form presented here.

The possibility remains that we may have not detected the binding of H17 to canonical human or avian receptors using the soluble protein in vitro, because it is plausible that a stronger interaction may occur through receptor clustering in vivo. It is also possible that H17 may bind to canonical influenza receptors very weakly, below the level of our detection. However, together with the extensive amino acid changes in the receptor binding site of H17 protein, it is likely that the putative bat influenza virus has acquired a different (possibly protein-based) receptor. There are many examples of closely related viruses that switch between protein and SA receptors (e.g., paramyxoviruses). The most common type of paramyxovirus attachment protein, called hemagglutinin-neuraminidase (HN), which is found on viruses such as Newcastle disease virus and human parainfluenza virus 3, recognizes the SA receptors. The structures of the globular heads of HN proteins display a conserved β sheet propeller motif, which was identified originally in influenza virus NA, and the SA binding site is located in the central cavity of the proteins. Unlike HN, the hemagglutinin (H) of measles virus (MV), which also belongs to the Paramyxoviridae family, possesses an inactivated SA receptor binding site and recognizes specific proteins, such as signal lymphocyte-activating molecule (SLAM), CD46 and nectin-4 (Mühlebach et al., 2011; Naniche et al., 1993; Tatsuo et al., 2000). The structure of the globular heads of H protein still reveals a conserved β sheet propeller motif, and the specific protein receptors bind to the side part of H protein with different orientations (Zhang et al., 2013). In particular, the immunoglobulin (Ig)-like SLAM molecule binds the H proteins mainly through interactions between two β sheets (Figure 7A). Interestingly, the bat influenza virus H17 and N10 proteins have similar Ig-like fold elements (Figure 7), which possibly provide the β sheets to interact with the protein-based receptors. If the H17 protein should lose its trimerization state and expose its Ig-like fold element, then it might bind a specific protein receptor. In this case, the bat influenza virus would abrogate the need for an active N10.

Another interesting characteristic of the H17 protein is its trypsin susceptibility and instability. Cleaved HA protein can activate its membrane fusion function under low-pH conditions, accompanied by enzymatic cleavage and large conformational rearrangements. However, H17 exhibited trypsin susceptibility

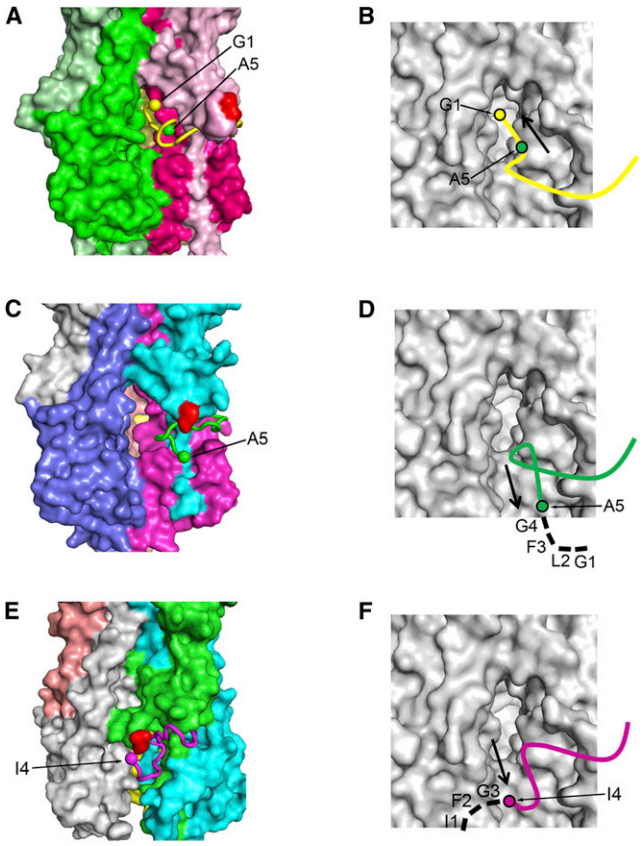

Figure 5. Exposed Fusion Peptide in the Cleavage Site of the H17 Structure

(A) Surface diagram of the fusion peptide in the representative H3 structure. The fusion peptide inserts into the cavity near the cleavage site.

(B, D, and F) Model diagrams of different conformations of the fusion peptide in the H3, H17, and HEF structures. The black arrow represents the direction of the fusion peptide. The dashed lines represent the residues that are not seen. Residues G1, L2, F3, and G4 are omitted in the H17 structure due to poor electrostatic mapping. In HEF structure, the omitted residues are I1, F2, and G3.

(C) Surface diagram of the fusion peptide in the H17 structure. The fusion peptide is exposed away from the cavity.

(E) Surface diagram of the fusion peptide in the HEF structures of influenza C viruses. The fusion peptide is partially exposed away from the cavity.

See also Figures S4 and S5.

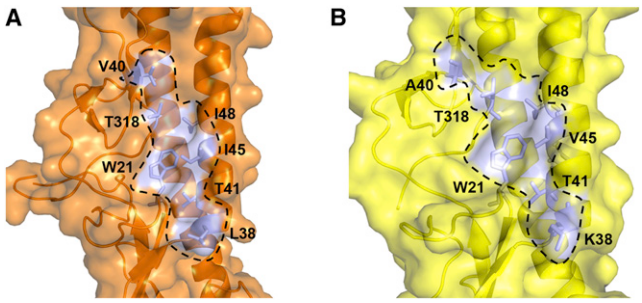

Figure 6. Conserved Hydrophobic Groove in H17 Protein Reveals the Structure Basis of Binding with the Broad Neutralizing Antibody FI6

(A and B) Surface representation of the F subdomains of 09H1 HA (A) and H17 HA (B) with selected side chains that contribute to the conserved hydrophobic groove. The approximate boundaries of the hydrophobic grooves are indicated by the black lines. Although the residues contributing to the hydrophobic groove are moderately different between 09H1 and H17, similar hydrophobic grooves guarantee the binding potential by the antibody FI6.

at high pH (8.0), similar to the low-pH-cleaved HA proteins, suggesting that H17 may utilize a different membrane-fusion mechanism than other HA subtypes. Currently, we hypothesize that H17 may not enter cells through endocytosis into the endosome for low-pH-induced membrane fusion. Instead, the fusion might occur on the cell surface at neutral pH.

Consistent with the observed trypsin susceptibility, H17 displayed a lower thermostability and may easily undergo a conformational change to expose enzymatic sites for trypsin digestion. Because the protein appears to be 50% unfolded at 37°C, it would not fare well in a fevered person but would fare well in a nonfebrile person. Interestingly, the body temperature of the bats can decrease to the same temperature as the environment when they hibernate in the winter. Thus, the H17N10 virus would still fare well in the bat because the H17 protein was more stable in cold temperature. Structural analysis of the cleavage site of the H17 structure reveals that the fusion peptide is exposed due to tighter trimerization of H17 compared to other HAs, which precludes fusion peptide insertion into the cavity. In contrast, in all other solved cleaved HA structures, the fusion peptides form a hydrophobic core at the center of the HA trimer. Thus, lack of this hydrophobic core may reduce the stability of the H17 protein.

In conclusion, our functional and structural characterization of the bat-derived influenza-like virus H17 protein revealed several special features: lack of SA receptor binding, trypsin susceptibility, thermoinstability, and a distorted putative SA binding site. Our group and the Wilson group recently reported that the paired bat-derived N10 protein lacks NA activity and also has a distorted pseudo-SA binding site, despite possessing an overall canonical NA fold (Li et al., 2012; Zhu et al., 2012). Taken together, these data raise further questions about how the bat influenza-like virus enters and is released from host cells.

EXPERIMENTAL PROCEDURES

Cloning, Expression, and Purification

The preparation procedures for 09H1 (2009 pH1N1), H2 (1957 pandemic Singapore strain, A/Singapore/1/1957 H2N2), H3 (1968 pandemic Hong Kong strain, A/Hong Kong/1/1968 H3N2), H5 (strain A/BhGoose/QH/1/05 H5N1), H16 (strain A/Black-headed Gull/Sweden/2/99 H16N3), and H17 proteins follow previously described methods (Zhang et al., 2010). Briefly, for H17, the complimentary DNA sequence encoding the ectodomain (residues 11–329 [HA1] and 1–176 [HA2]; based on H3 numbering) of influenza A/little yellow-shouldered bat/Guatemala/060/2010(H17N10) HA protein H17 was cloned into the pFastBac1 baculovirus transfer vector. A gp67 signal peptide was inserted at the N terminus to facilitate protein secretion, followed by a thrombin cleavage site, a foldon sequence, and a His-tag (Zhang et al., 2010). Recombinant HA protein secreted into the cell culture media contains additional plasmid-encoded residues at both the N terminus (ADLQ) and C terminus (R*LVPRGS*PGSGYIPEAPRDGQAYVRKDGEWVLLSTFLG**HHHHHH**, where the sequence in italics is the thrombin site, the foldon sequence is underlined, and the His-tag is bold). Transfection and virus amplification were performed according to the Bac-to-Bac baculovirus expression system

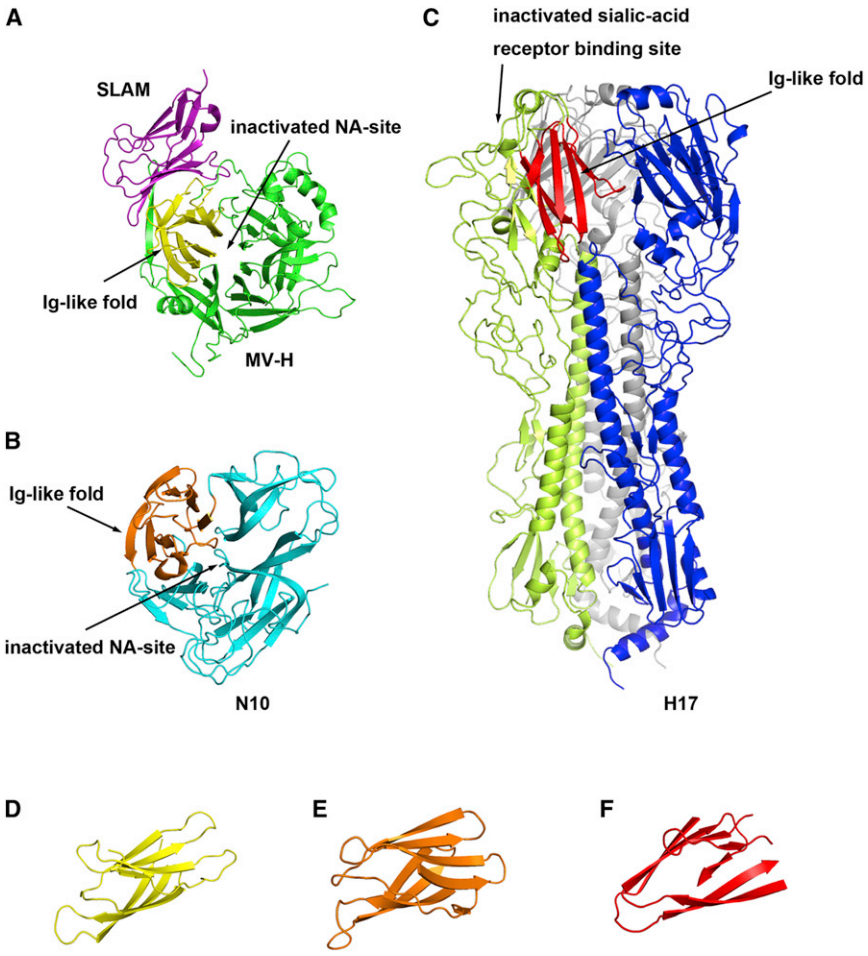

Figure 7. Structural Comparison of the Ig-like Fold Elements among Measles Virus H Protein, N10, and H17

(A) Cartoon diagram of the complex structure of measles virus H (MV-H) protein and its receptor SLAM. The Ig-like SLAM molecule binds the H proteins mainly through the interaction between two β sheets.

(B) Cartoon diagram of the structure of the bat influenza N10 molecule. N10 has a similar Ig-like fold, which might provide the β sheet to interact with a protein receptor.

(C) Cartoon diagram of the structure of the H17 protein. H17 has similar Ig-like fold in the globular domain, which might provide the β sheet to interact with a protein receptor.

(D–F) The Ig-like fold elements from MV-H, N10, and H17 are picked up and shown alone. Both the N10 and H17 molecules have a β sheet similar to the MV-H protein.

manual (Invitrogen). Hi5 cells were infected with high-titer recombinant baculovirus. After incubation for 2 days, cells were removed by centrifugation. The supernatant was filtered and loaded onto a 5 ml HisTrap HP column (GE Healthcare). The column was washed with 20 mM imidazole and then HA was eluted using 300 mM imidazole. Fractions containing H17 protein were pooled and dialyzed against 10 mM Tris-HCl (pH 8.0) and 40 mM NaCl and then subjected to ion-exchange chromatography using a Mono Q 4.6/100 PE column (GE Healthcare). Next, the protein was digested with thrombin (3 U/mg protein) overnight at 4°C and further purified by gel filtration chromatography using a Superdex200 10/300 GL column (GE Healthcare) with a buffer of 20 mM Tris-HCl (pH 8.0) and 50 mM NaCl. High-purity HA fractions were concentrated using a membrane concentrator with a molecular weight cutoff of 10 kDa (Millipore).

Crystallization, Data Collection, and Structure Determination

H17 crystals were grown by the sitting drop vapor diffusion method. Protein (1 μl at 10 mg/ml) in 20 mM Tris (pH 8.0) and 50 mM NaCl was mixed with 1 μl reservoir solution (0.1 M sodium citrate tribasic dehydrate (pH 5.0) and 30% v/v Jeffamine ED-2001 [pH 7.0]). H17 crystals were cryoprotected in mother liquor by the addition of 20% glycerol before being flash-cooled at 100 K. Diffraction data for H17 were collected at SSRF beamline BL17U. The collected intensities were indexed, integrated, corrected for absorption, and then scaled and merged using HKL2000 (Otwinowski and Minor, 1997). The H17 structure was solved by molecular replacement using Phaser (Read, 2001) from the CCP4 program suite (Collaborative Computational Project, Number 4, 1994) with the structure of H16 (PDB ID code: 4F23) as the search model. The initial model was refined by rigid-body refinement using REFMAC5 (Murshudov et al., 1997), and extensive model building was performed using COOT (Emsley and Cowtan, 2004). Further rounds of refinement were performed using the phenix.refine program implemented in the PHENIX package (Adams et al., 2010) with energy minimization, isotropic ADP refinement, and bulk solvent modeling. Final statistics for the H17 structure are represented in Table S2. The stereochemical quality of the final model was assessed with the program PROCHECK (Laskowski et al., 1993).

Trypsin Susceptibility Assays

Purified HA0 in a buffer of pH 8.0 (20 mM Tris-HCl and 50 mM NaCl) was concentrated to 1 mg/ml and 10 μl protein was added to each tube. TPCK-treated trypsin (Sigma) was added to each sample to a final concentration of 2.5 μg/ml and the digestion was performed at 37°C. At time points of 5, 10, 20, 40, 80, and 120 min, the digestion was stopped by adding a 5 × SDS loading buffer containing DTT and boiled for 5 min. Samples were then loaded onto a 12% SDS-PAGE. For the low-pH digestion experiment, H3 HA0 was first digested with trypsin at 4°C overnight and the extra trypsin was removed by gel filtration. Then, cleaved H3 and H17 HA0 were incubated at pH 5.0 for 30 min by using sodium acetate (pH 4.5) to adjust the pH. Finally, the trypsin digestion of the low-pH-treated H3 and H17 was analyzed as described above.

MDCK Cell Binding Assays

The cell binding assays were performed in 96-well plates. When the density of the MDCK cells in the wells reached 90% coverage, the plate was washed with PBST buffer (PBS with 0.05% Tween 20) three times. His-tagged H17 or H5 HA protein (2, 4, 8, 12, 16, or 20 μg) was then added to each well. Each concentration was analyzed twice in triplicate. After incubation at 37°C for 1 hr, the plate was washed three times with PBST buffer. Mouse his-tag antibody was added to each well at a 1:1000 dilution and the plate was incubated for 45 min. Then, the plate was washed and incubated at 37°C for 30 min with horseradish-peroxidase-conjugated anti-mouse antibody at a dilution of 1:200. Peroxidase activity was detected using 3, 3′, 5, 5′-tetramethylbenzidine and the reaction was stopped by adding 0.2 M H_2SO_4. Absorbance was measured at an optical density of 450 nm. The experiment was repeated three times.

CD Experiments

The thermostabilities of the 09H1, H2, H3, H5, H16, and H17 proteins were tested by CD spectroscopy. CD spectra were measured from 20°C–94°C on

a ChiraScan spectropolarimeter equipped with a water-circulating cell holder. The spectra were obtained in 20 mM Tris (pH 8.0) and 50 mM NaCl using a 1 cm optical path length cell. The protein concentration was 25 μg/ml. The temperature was increased by 1°C/min. Thermal denaturation curves were determined by monitoring the CD value at 218 nm. The data were analyzed using Origin.8 software.

SPR Measurements and Affinity Analysis

The affinity and kinetics of the binding of soluble HAs to receptor analogs were measured at 25°C on a BIAcore 3000 machine with streptavidin chips (SA chips, BIAcore) by SPR. The protein was purified by gel filtration with PBST buffer (PBS buffer with 0.005% Tween 20, pH 7.4), which was used for all measurements. Two biotinylated receptor analogs, the α-2,6 glycans (6′S-Di-LN: Neu5Aca2-6[Galb1-4GlcNAcb1-3]2b-SpNH-LC-LC-Biotin) and the α-2,3 glycans (3′S-Di-LN: Neu5Aca2-3[Galb1-4GlcNAcb1-3]2b-SpNH-LC-LC-Biotin) were kindly provided by the Consortium for Functional Glycomics (Scripps Research Institute, Department of Molecular Biology, La Jolla, CA, USA). The α-2,6 glycans and α-2,3 glycans were immobilized on the CM5 chip with 450 response units. H17 HA protein at 100, 50, 25, 12.5, 6.25, 3.125, or 0 μM flowed through the chip and the response unit was measured. H5 HA protein (2.5 μM) was used as the positive control. The data were analyzed with BIAcore software (BIAevaluation version 4.1) using a 1:1 Langumuir binding mode.

Glycan Microarray

The microarray analyses were performed by applying the protein to the array at 200 μg/ml and detecting with a His antibody labeled with Alexa488. The experiments were performed in replicates of six at Core H of the Consortium for Functional Glycomics using a version 5.0 CFG array consisting of 611 glycans. The highest and lowest points from each set of six replicates were removed, so the average is of four values rather than six. This eliminates some of the false hits that contain a single very high or low point.

N-Terminal Sequencing

The crystal samples were applied to SDS-PAGE and subsequently transferred to polyvinylidene fluoride (PVDF) membrane at 200 mA for 1 hr. The PVDF blot membrane was stained for 5 min in CBB R250 staining solution (0.1% CBB R250, 10% acetic acid, 40% methanol in Milli-Q water) and destained with destaining solution (10% acetic acid, 40% methanol in Milli-Q water) under visual control until protein bands were well visible. The PVDF membrane was dried and bands of interest were cut for the N-terminal sequencing with the Edman degradation method using PROCISE491 (America Applied Biosystems).

Analytical Ultracentrifugation

Sedimentation velocity experiments were done at 20°C in a Beckman Optima XL-I analytical ultracentrifuge (An50Ti rotor). Double-sector cells with charcoal-filled Epon centerpieces were loaded with 400 μl protein solution in 20 mM Tris-HCl (pH 8.0) and 150 mM NaCl. Data were collected at 180,000 × *g* with interference and absorbance optical detection. The program SEDFIT was used for data analysis (http://www.analyticalultracentrifugation.com).

ACCESSION NUMBERS

The H17 structure reported in this paper has been deposited in the Protein Data Bank under ID code 4H32.

SUPPLEMENTAL INFORMATION

Supplemental Information includes five figures and three tables and can be found with this article online at http://dx.doi.org/10.1016/j.celrep.2013.01.025.

LICENSING INFORMATION

ACKNOWLEDGMENTS

This work was supported by the National 973 Project (grant 2011CB504703), the China National Grand S&T Special Project (grant 2013ZX10004-611), and the National Natural Science Foundation of China (NSFC; grant 81021003). G.F.G. is a leading principal investigator of the NSFC Innovative Research Group. Assistance by the staff at the Shanghai Synchrotron Radiation Facility (SSRF-beamline 17U) is acknowledged. The authors would also like to acknowledge The Consortium for Functional Glycomics funded by the NIGMS GM62116 for support of the glycan array analysis, especially Dr. David Smith and James Heimburg-Molinaro.

Received: October 17, 2012
Revised: December 18, 2012
Accepted: January 22, 2013
Published: February 21, 2013

REFERENCES

Adams, P.D., Afonine, P.V., Bunkóczi, G., Chen, V.B., Davis, I.W., Echols, N., Headd, J.J., Hung, L.W., Kapral, G.J., Grosse-Kunstleve, R.W., et al. (2010). PHENIX: a comprehensive Python-based system for macromolecular structure solution. Acta Crystallogr. D Biol. Crystallogr. *66*, 213–221.

Air, G.M. (1981). Sequence relationships among the hemagglutinin genes of 12 subtypes of influenza A virus. Proc. Natl. Acad. Sci. USA *78*, 7639–7643.

Bullough, P.A., Hughson, F.M., Skehel, J.J., and Wiley, D.C. (1994). Structure of influenza haemagglutinin at the pH of membrane fusion. Nature *371*, 37–43.

Chen, J., Lee, K.H., Steinhauer, D.A., Stevens, D.J., Skehel, J.J., and Wiley, D.C. (1998). Structure of the hemagglutinin precursor cleavage site, a determinant of influenza pathogenicity and the origin of the labile conformation. Cell *95*, 409–417.

Collaborative Computational Project, Number 4. (1994). The CCP4 suite: programs for protein crystallography. Acta Crystallogr. D Biol. Crystallogr. *50*, 760–763.

Corti, D., Voss, J., Gamblin, S.J., Codoni, G., Macagno, A., Jarrossay, D., Vachieri, S.G., Pinna, D., Minola, A., Vanzetta, F., et al. (2011). A neutralizing antibody selected from plasma cells that binds to group 1 and group 2 influenza A hemagglutinins. Science *333*, 850–856.

Eisen, M.B., Sabesan, S., Skehel, J.J., and Wiley, D.C. (1997). Binding of the influenza A virus to cell-surface receptors: structures of five hemagglutinin-sialyloligosaccharide complexes determined by X-ray crystallography. Virology *232*, 19–31.

Ekiert, D.C., Bhabha, G., Elsliger, M.A., Friesen, R.H., Jongeneelen, M., Throsby, M., Goudsmit, J., and Wilson, I.A. (2009). Antibody recognition of a highly conserved influenza virus epitope. Science *324*, 246–251.

Ekiert, D.C., Friesen, R.H., Bhabha, G., Kwaks, T., Jongeneelen, M., Yu, W., Ophorst, C., Cox, F., Korse, H.J., Brandenburg, B., et al. (2011). A highly conserved neutralizing epitope on group 2 influenza A viruses. Science *333*, 843–850.

Emsley, P., and Cowtan, K. (2004). Coot: model-building tools for molecular graphics. Acta Crystallogr. D Biol. Crystallogr. *60*, 2126–2132.

Gambaryan, A.S., Tuzikov, A.B., Piskarev, V.E., Yamnikova, S.S., Lvov, D.K., Robertson, J.S., Bovin, N.V., and Matrosovich, M.N. (1997). Specification of receptor-binding phenotypes of influenza virus isolates from different hosts using synthetic sialylglycopolymers: non-egg-adapted human H1 and H3 influenza A and influenza B viruses share a common high binding affinity for 6′-sialyl(N-acetyllactosamine). Virology *232*, 345–350.

Gamblin, S.J., and Skehel, J.J. (2010). Influenza hemagglutinin and neuraminidase membrane glycoproteins. J. Biol. Chem. *285*, 28403–28409.

Gao, G.F., and Sun, Y. (2010). It is not just AIV: from avian to swine-origin influenza virus. Sci. China Life Sci. *53*, 151–153.

Garten, W., and Klenk, H.D. (1999). Understanding influenza virus pathogenicity. Trends Microbiol. *7*, 99–100.

Guan, Y., Vijaykrishna, D., Bahl, J., Zhu, H., Wang, J., and Smith, G.J. (2010). The emergence of pandemic influenza viruses. Protein Cell *1*, 9–13.

Harrison, S.C. (2008). Viral membrane fusion. Nat. Struct. Mol. Biol. *15*, 690–698.

Laskowski, R.A., Macarthur, M.W., Moss, D.S., and Thornton, J.M. (1993). PROCHECK: a Program to Check the Stereochemical Quality of Protein Structures. J. Appl. Crystallogr. *26*, 283–291.

Li, Q., Sun, X., Li, Z., Liu, Y., Vavricka, C.J., Qi, J., and Gao, G.F. (2012). Structural and functional characterization of neuraminidase-like molecule N10 derived from bat influenza A virus. Proc. Natl. Acad. Sci. USA *109*, 18897–18902.

Liu, D., Liu, X., Yan, J., Liu, W.J., and Gao, G.F. (2009). Interspecies transmission and host restriction of avian H5N1 influenza virus. Sci. China C Life Sci. *52*, 428–438.

Lu, X., Shi, Y., Gao, F., Xiao, H., Wang, M., Qi, J., and Gao, G.F. (2012). Insights into avian influenza virus pathogenicity: the hemagglutinin precursor HA0 of subtype H16 has an alpha-helix structure in its cleavage site with inefficient HA1/HA2 cleavage. J. Virol. *86*, 12861–12870.

Medina, R.A., and García-Sastre, A. (2011). Influenza A viruses: new research developments. Nat. Rev. Microbiol. *9*, 590–603.

Mühlebach, M.D., Mateo, M., Sinn, P.L., Prüfer, S., Uhlig, K.M., Leonard, V.H., Navaratnarajah, C.K., Frenzke, M., Wong, X.X., Sawatsky, B., et al. (2011). Adherens junction protein nectin-4 is the epithelial receptor for measles virus. Nature *480*, 530–533.

Murshudov, G.N., Vagin, A.A., and Dodson, E.J. (1997). Refinement of macromolecular structures by the maximum-likelihood method. Acta Crystallogr. D Biol. Crystallogr. *53*, 240–255.

Naniche, D., Varior-Krishnan, G., Cervoni, F., Wild, T.F., Rossi, B., Rabourdin-Combe, C., and Gerlier, D. (1993). Human membrane cofactor protein (CD46) acts as a cellular receptor for measles virus. J. Virol. *67*, 6025–6032.

Neumann, G., Noda, T., and Kawaoka, Y. (2009). Emergence and pandemic potential of swine-origin H1N1 influenza virus. Nature *459*, 931–939.

Nobusawa, E., Aoyama, T., Kato, H., Suzuki, Y., Tateno, Y., and Nakajima, K. (1991). Comparison of complete amino acid sequences and receptor-binding properties among 13 serotypes of hemagglutinins of influenza A viruses. Virology *182*, 475–485.

Otwinowski, Z., and Minor, W. (1997). Processing of X-ray diffraction data collected in oscillation mode. Methods Enzymol. *276*, 307–326.

Read, R.J. (2001). Pushing the boundaries of molecular replacement with maximum likelihood. Acta Crystallogr. D Biol. Crystallogr. *57*, 1373–1382.

Rosenthal, P.B., Zhang, X., Formanowski, F., Fitz, W., Wong, C.H., Meier-Ewert, H., Skehel, J.J., and Wiley, D.C. (1998). Structure of the haemagglutinin-esterase-fusion glycoprotein of influenza C virus. Nature *396*, 92–96.

Sauter, N.K., Bednarski, M.D., Wurzburg, B.A., Hanson, J.E., Whitesides, G.M., Skehel, J.J., and Wiley, D.C. (1989). Hemagglutinins from two influenza virus variants bind to sialic acid derivatives with millimolar dissociation constants: a 500-MHz proton nuclear magnetic resonance study. Biochemistry *28*, 8388–8396.

Skehel, J.J., and Wiley, D.C. (2000). Receptor binding and membrane fusion in virus entry: the influenza hemagglutinin. Annu. Rev. Biochem. *69*, 531–569.

Skehel, J.J., Bayley, P.M., Brown, E.B., Martin, S.R., Waterfield, M.D., White, J.M., Wilson, I.A., and Wiley, D.C. (1982). Changes in the conformation of influenza virus hemagglutinin at the pH optimum of virus-mediated membrane fusion. Proc. Natl. Acad. Sci. USA *79*, 968–972.

Sui, J., Hwang, W.C., Perez, S., Wei, G., Aird, D., Chen, L.M., Santelli, E., Stec, B., Cadwell, G., Ali, M., et al. (2009). Structural and functional bases for broad-spectrum neutralization of avian and human influenza A viruses. Nat. Struct. Mol. Biol. *16*, 265–273.

Sun, Y., Shi, Y., Zhang, W., Li, Q., Liu, D., Vavricka, C., Yan, J., and Gao, G.F. (2010). In silico characterization of the functional and structural modules of the hemagglutinin protein from the swine-origin influenza virus A (H1N1)-2009. Sci. China Life Sci. *53*, 633–642.

Takemoto, D.K., Skehel, J.J., and Wiley, D.C. (1996). A surface plasmon resonance assay for the binding of influenza virus hemagglutinin to its sialic acid receptor. Virology *217*, 452–458.

Tatsuo, H., Ono, N., Tanaka, K., and Yanagi, Y. (2000). SLAM (CDw150) is a cellular receptor for measles virus. Nature *406*, 893–897.

Tong, S., Li, Y., Rivailler, P., Conrardy, C., Castillo, D.A., Chen, L.M., Recuenco, S., Ellison, J.A., Davis, C.T., York, I.A., et al. (2012). A distinct lineage of influenza A virus from bats. Proc. Natl. Acad. Sci. USA *109*, 4269–4274.

Webster, R.G., Bean, W.J., Gorman, O.T., Chambers, T.M., and Kawaoka, Y. (1992). Evolution and ecology of influenza A viruses. Microbiol. Rev. *56*, 152–179.

Weis, W., Brown, J.H., Cusack, S., Paulson, J.C., Skehel, J.J., and Wiley, D.C. (1988). Structure of the influenza virus haemagglutinin complexed with its receptor, sialic acid. Nature *333*, 426–431.

Xuan, C., Shi, Y., Qi, J., Zhang, W., Xiao, H., and Gao, G.F. (2011). Structural vaccinology: structure-based design of influenza A virus hemagglutinin subtype-specific subunit vaccines. Protein Cell *2*, 997–1005.

Zhang, W., Qi, J., Shi, Y., Li, Q., Gao, F., Sun, Y., Lu, X., Lu, Q., Vavricka, C.J., Liu, D., et al. (2010). Crystal structure of the swine-origin A (H1N1)-2009 influenza A virus hemagglutinin (HA) reveals similar antigenicity to that of the 1918 pandemic virus. Protein Cell *1*, 459–467.

Zhang, X., Lu, G., Qi, J., Li, Y., He, Y., Xu, X., Shi, J., Zhang, C.W., Yan, J., and Gao, G.F. (2013). Structure of measles virus hemagglutinin bound to its epithelial receptor nectin-4. Nat. Struct. Mol. Biol. *20*, 67–72.

Zhu, X., Yang, H., Guo, Z., Yu, W., Carney, P.J., Li, Y., Chen, L.M., Paulson, J.C., Donis, R.O., Tong, S., et al. (2012). Crystal structures of two subtype N10 neuraminidase-like proteins from bat influenza A viruses reveal a diverged putative active site. Proc. Natl. Acad. Sci. USA *109*, 18903–18908.